NASA TECHNICAL NOTE

NASA TN D-5651

THERMAL RADIATIVE PROPERTY MEASUREMENTS USING CYCLIC RADIATION

by John R. Jack and Ernie W. Spisz

Lewis Research Center
Cleveland, Ohio

NATIONAL AERONAUTICS AND SPACE ADMINISTRATION • WASHINGTON, D. C. • MARCH 1970

1. Report No. NASA TN D-5651	2. Government Accession No.	3. Recipient's Catalog No.
4. Title and Subtitle THERMAL RADIATIVE PROPERTY MEASUREMENTS USING CYCLIC RADIATION		5. Report Date March 1970 6. Performing Organization Code
7. Author(s) John R. Jack and Ernie W. Spisz		8. Performing Organization Report No. E-5356
9. Performing Organization Name and Address Lewis Research Center National Aeronautics and Space Administration Cleveland, Ohio 44135		10. Work Unit No. 124-09 11. Contract or Grant No.
12. Sponsoring Agency Name and Address National Aeronautics and Space Administration Washington, D.C. 20546		13. Type of Report and Period Covered Technical Note 14. Sponsoring Agency Code

15. Supplementary Notes

16. Abstract

An experimental technique that determines simultaneously the total hemispherical emittance, solar absorptance, and the absorptance-emittance ratio for various materials over a substantial temperature range is discussed. The method is based upon comparing the temperature response of a thin, flat, isothermal sample to a sinusoidal perturbation of an imposed incident radiation. An experimental validation of the method is presented along with experimental thermal radiative property data for a variety of materials at temperatures ranging from 150 to 600 K. Twelve metals, a Z-93 coating, a black velvet paint, and a composite material (a CdS solar cell) were investigated to demonstrate the capabilities and the general utility and versatility of the cyclic radiation method for determining thermal radiative properties.

17. Key Words *(Suggested by Author(s))* Thermal radiative properties	18. Distribution Statement Unclassified - unlimited

19. Security Classif. (of this report) Unclassified	20. Security Classif. (of this page) Unclassified	21. No. of Pages 35	22. Price* $3.00

*For sale by the Clearinghouse for Federal Scientific and Technical Information Springfield, Virginia 22151

THERMAL RADIATIVE PROPERTY MEASUREMENTS USING CYCLIC RADIATION

by John R. Jack and Ernie W. Spisz

Lewis Research Center

SUMMARY

An experimental technique that determines simultaneously the total hemispherical emittance, solar absorptance, and the absorptance-emittance ratio for various materials over a substantial temperature range is discussed. The method is based upon comparing the temperature response of a thin, flat, isothermal sample to a sinusoidal perturbation of an imposed incident radiation. An experimental validation of the method is presented along with experimental thermal radiative property data for a variety of materials at temperatures ranging from 150 to 600 K. Twelve metals, a Z-93 coating, a black velvet paint, and a composite material (a CdS solar cell) were investigated to demonstrate the capabilities and the general utility and versatility of the cyclic radiation method for determining thermal radiative properties.

INTRODUCTION

The design of space vehicles and space equipment requires accurate total radiative property data on all types of materials over a wide range of environmental conditions. This need stems from the fact that passive spacecraft temperature control is generally achieved by a radiation heat exchange between spacecraft components and the space environment. Neither existing experimental data nor theoretical predictions are adequate to fill this need. Therefore, the designers responsible for spacecraft thermal control must rely completely upon accurate experimental determinations of thermal radiative properties that satisfy the required combination of thermal and environmental boundary conditions.

Various techniques are available for the determination of thermal radiative properties; most of which require a separate experiment for each radiative property desired. Of the many methods available, all can be classified as either a thermal or an optical

technique. However, each method has associated with it experimental difficulties and limitations.

Thermal methods are generally calorimetric and determine total radiative properties either by equilibrium or transient temperature measurements. The calorimetric approach has inherent errors, such as accurate temperature measurement, heat leaks, background radiation, and convective heat-transfer effects; all of which can significantly affect the experimental results (ref. 1). This is especially true at low temperature levels, where the heat transferred by radiation is small.

With optical methods, the spectral reflectance is measured over the appropriate spectral range and the desired thermal radiative property calculated. Such calculations are lengthy and arduous, but more importantly, the spectral reflectance method involves a series of assumptions related to the equipment and sample characteristics such as specularity, angular dependency, and polarization (ref. 2). In addition, although the reflectance can be measured accurately, the error in the calculated thermal radiative properties α, ϵ can be very large for highly reflecting materials. For example, polished aluminum with a reflectance of 0.98 ± 0.005 at a wavelength of 10 micrometers yields an error in spectral emittance of 25 percent.

Thus, although some information on the thermal radiation characteristics of materials is available, the data are, in general, not completely reproducible from specimen to specimen nor from source to source for the same material. This, coupled with the facts that our basic understanding of the physical phenomena is not sufficient to permit reliable theoretical predictions and that experimental techniques and measurements have not reached a completely satisfactory level, describes a technical situation in need of an innovation.

A new measuring technique based upon a cyclic perturbation of the incident radiation was initiated in the spring of 1966 at the NASA Lewis Research Center. A mathematical analysis of this new technique was first presented in reference 3. Previously obtained data using this method have been reported in references 4 to 8. The intent of this report is to summarize in a single, readily available publication the results obtained to date with the cyclic radiation technique. The present report therefore contains the following: (1) a complete analysis of the technique along with a discussion of its possible errors and its advantages and disadvantages, (2) an experimental validation of the method, and finally (3) experimental thermal radiative property data obtained with this method over a range of temperatures (150 to 600 K) and for a variety of materials. Metals, coatings, and a composite material (a CdS solar cell) were investigated, utilizing the cyclic technique, to demonstrate its capabilities and its general utility. In addition, preliminary data are included on the specific heat of a paint as obtained by the cyclic radiation technique.

THEORETICAL BASIS OF METHOD

The cyclic method for measuring the normal absorptance and hemispherical emittance of surfaces is based on the temperature response of a thin, flat, isothermal model exposed to radiation (either solar or thermal) which is varied in a prescribed periodic manner after a steady-state isothermal model temperature T_m has been established. The instantaneous heat-balance equation governing the model temperature is given by

$$wc_p \frac{dT}{dt} = \alpha A_s I(t) + q - 2\epsilon\sigma A_s T^4 \tag{1}$$

where q is the net heat absorbed (or lost) by the sample from all sources other than that from the incident radiation $I(t)$ which can have a variety of functional forms such as step, ramp, or sinusoidal. (All symbols are defined in the appendix.) Now if it is specified that the incident radiation vary in a convenient, periodic fashion with small amplitude about a mean level, the variation of the sample temperature about its equilibrium value T_m will be small, and equation (1) can be linearized with respect to the equilibrium temperature as

$$w\left[c_p + \left(\frac{dc_p}{dT}\right)_{T_m} (T - T_m)\right]\frac{d(T - T_m)}{dt} = \left[\alpha + \left(\frac{d\alpha}{dT}\right)_{T_m} (T - T_m)\right] A_s I(t)$$

$$+ \left[q + \left(\frac{dq}{dT}\right)_{T_m} (T - T_m)\right] - 2\sigma A_s \left[4\epsilon T_m^3 T - 3\epsilon T_m^4 + T_m^4 \left(\frac{d\epsilon}{dT}\right)_{T_m} (T - T_m)\right] \tag{2}$$

Since the model temperature is only perturbed, it is reasonable and expedient to assume, in each case, that the product of the temperature derivative and the delta temperature is small and can be neglected in the heat-balance equation.

For a sinusoidal variation of the imposed radiant intensity

$$I(t) = I_o + i \sin \omega t = I_o(1 + j \sin \omega t) \tag{3}$$

equation (2) can be approximated as

$$wc_p \frac{d(T - T_m)}{dt} = \alpha A_s j I_o \sin \omega t - 8\epsilon\sigma A_s T_m^3 (T - T_m) \tag{4}$$

Casting the original differential equation in this form illustrates one of the major assets of the cyclic approach for measuring thermal radiative properties. Most calorimetric methods must either assume that the heat-loss term in equation (1) is negligible or include a means to correct for it. In some instances the correction can be of the same magnitude as the terms of interest. In the cyclic technique the steady-state heat loss is unimportant because it is automatically accounted for by the mean temperature T_m, which is an accurately measurable quantity.

A sinusoidal variation of incident radiation is used since it is one of the simplest functions to handle analytically and, in addition, provides a convenient closed-form solution. The solution of equation (4) then becomes

$$T - T_m = A \sin(\omega t - \varphi) + Ce^{-t/\theta'} \tag{5}$$

where

$$A = \frac{\alpha j I_o A_s}{\omega c_p w} \sin \varphi \tag{5a}$$

$$C = \frac{\dfrac{jI_o}{8\sigma T_m^3} (\omega\theta') \dfrac{\alpha}{\epsilon}}{1 + (\omega\theta')^2} \tag{5b}$$

$$\theta' = \frac{wc_p}{8\epsilon\sigma T_m^3 A_s} \tag{5c}$$

$$\varphi = \tan^{-1} \omega\theta' \tag{5d}$$

Equation (5) is the complete solution of the differential equation. The constant C is determined from the initial condition: $T = T_m$ at $t = 0$. The last term of the solution decays exponentially with time and, after a sufficiently long interval, becomes negligible compared with the periodic term. Eventually, the sample temperature varies only in a steady-state sinusoidal fashion. Figure 1 illustrates graphically the variation of the model temperature on exposure to a sinusoidally varying incident radiation. It is noted that the sample temperature is out of phase with the incident radiation and lags behind it by an angle φ which varies from 0^o at a low frequency to (but never exceeding) 90^o for very high cyclic frequencies. The tangent of this angle is proportional to the cyclic frequency of the incident radiation as well as the time constant of the sample.

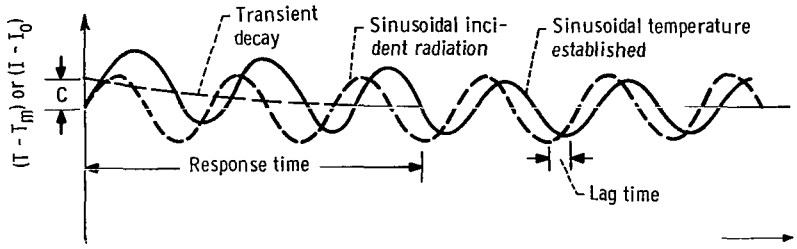

Figure 1. - Model temperature and incident radiation variations with time.

The steady-state periodic solution is of interest because it offers a very effective and convenient means for determining simultaneously the radiation properties of materials. Thus, by measuring the phase angle φ for a given frequency of incident radiation, the hemispherical emittance can be determined from

$$\epsilon = \frac{\omega c_p w}{8\sigma A_s T_m^3 \tan \varphi} \tag{6}$$

and the absorptance may be determined from a measurement of the temperature amplitude and phase angle

$$\alpha = \frac{\omega c_p w}{j I_o A_s} \frac{A}{\sin \varphi} \tag{7}$$

Several observations concerning the analysis are appropriate. It should be recognized immediately that the accuracy of the thermal radiative property data is directly dependent upon accurate values for the specific heat of the material. Generally, accurate specific-heat data are available for pure metals; however, accurate values are not readily available for alloys, coatings, paints, and composites.

The analysis assumes that the heat absorbed or lost by the sample q is independent of the sample temperature. This assumption must be looked at rather closely since it will affect the thermal radiative property determination especially at low temperature levels, where the amount of heat radiated away from the model is small. The concern here is the magnitude of the term $(dq/dT)_{T_m} (T - T_m)$ in equation (2). If this term is considered, the solution to the heat-balance equation is straightforward and similar to equation (5). The tangent of the phase angle is given by

$$\tan \varphi = \frac{\omega c_p \frac{w}{A_s}}{8\epsilon\sigma T_m^3 \pm \frac{K}{A_s}} \tag{8}$$

where the plus or minus sign is for a heat gain or loss and K is the heat-exchange temperature coefficient $K = (dq/dT)_{T_m}$

Solving for the true emittance yields

$$\epsilon_{true} = \frac{\omega c_p \frac{w}{A_s}}{8\sigma T_m^3 \tan \varphi} \pm \frac{K}{8\sigma A_s T_m^3} \tag{9}$$

so that the difference between the measured emittance and the true emittance is given by

$$\epsilon_{meas} - \epsilon_{true} = \mp \frac{K}{8\sigma A_s T_m^3} \tag{10}$$

It is noteworthy, however, that this difference is significantly less than that from the total heat-loss effect, which must be eliminated or accounted for in other methods for determining radiation properties. Furthermore, the effect of the heat-exchange temperature coefficient on the measured emittance can be minimized by using small-diameter, low-thermal-conductivity, low-emittance support wires or by using as large a sample surface area as possible.

Unlike the emittance, the absorptance determination is not affected by the heat-loss temperature coefficient since the effects of a heat loss do not appear independently in equation (7) but are included in the temperature amplitude and the phase angle. As a result the true absorptance is determined regardless of the heat-loss effect.

UNCERTAINTY ANALYSIS

An uncertainty analysis is useful to establish the capabilities and possible limitations of the cyclic technique and to indicate the major possible sources of error. In addition, the instrumentation requirements for securing accurate data over a range of conditions are established. In the cyclic technique, as in all techniques, the desired parameters (emittance and absorptance) are determined in terms of conveniently measur-

able parameters. The uncertainty analysis must therefore be made in terms of the estimated uncertainties inherent in these parameters.

The uncertainty in the emittance and absorptance as determined from equations (6) and (7) is given by (ref. 9)

$$\frac{\delta\epsilon}{\epsilon} = \left[\left(\frac{\delta w}{w}\right)^2 + \left(\frac{\delta A_s}{A_s}\right)^2 + \left(\frac{\delta c_p}{c_p}\right)^2 + \left(\frac{\delta\omega}{\omega}\right)^2 + \left(3\frac{\delta T_m}{T_m}\right)^2 + \left(\frac{\delta \tan\varphi}{\tan\varphi}\right)^2\right]^{1/2} \tag{11}$$

and

$$\frac{\delta\alpha}{\alpha} = \left[\left(\frac{\delta w}{w}\right)^2 + \left(\frac{\delta A_s}{A_s}\right)^2 + \left(\frac{\delta c_p}{c_p}\right)^2 + \left(\frac{\delta\omega}{\omega}\right)^2 + \left(\frac{\delta A}{A}\right)^2 + \left(\frac{\delta jI_o}{jI_o}\right)^2 + \left(\frac{\delta \sin\varphi}{\sin\varphi}\right)^2\right]^{1/2} \tag{12}$$

Considering each term separately, the uncertainty in w and A_s is due to the independent measurements of the weight and surface area of the samples. For samples of reasonable size and with proper equipment, the sample weight and area can easily be determined within an uncertainty of 0.01. The uncertainty in the applied cyclic frequency $\delta\omega/\omega$ can also be kept to within 0.01.

The uncertainty in the specific heat of the material is difficult to estimate. For most pure metallic elements, data are available (ref. 10) which are accurate to within an uncertainty of 0.02. However, for metal alloys, nonmetals, composites, or coatings, the uncertainty is considerably larger. For some materials, it may even be necessary to determine the specific heat, which for some materials may be obtained from the cyclic technique (see later discussion).

The uncertainty in the absolute temperature measurement is also difficult to estimate because of the thin samples (0.001 in.) and corresponding small-diameter thermocouple wire (0.001 in.), both of which are often necessary. The combination of thin samples, small-diameter wires, and the many possible errors which can be introduced as a result of transient conditions precludes an accurate calibration of the thermocouple system. A best estimate of the uncertainty associated with the temperature measurement, based upon steady-state calibration of a typical system, is 2 K.

The uncertainty in the temperature amplitude measurement $\delta A/A$ can be kept small because the measurement is relative and, with proper experimental technique, a high degree of resolution can be obtained over the range of the temperature perturbation. The uncertainty in temperature amplitude measurement is estimated to be within 0.01.

Similarly, the uncertainty in the intensity amplitude factor can be kept quite small because the measurement is also relative and the resolution can be made quite large.

The uncertainty associated with this parameter is also estimated to be within 0.01.

The final and most important parameter is the measurement of the phase angle between the sample temperature and the imposed radiant intensity. The phase angle can be measured by a number of different methods; however, it is doubtful that this measurement can be made with an accuracy of better than 1°. The uncertainty associated with the determination of $\tan \varphi$ and $\sin \varphi$ required for an emittance and an absorptance determination is

$$\frac{\delta \tan \varphi}{\tan \varphi} = \frac{2\delta\varphi}{\sin 2\varphi} \tag{13}$$

$$\frac{\delta \sin \varphi}{\sin \varphi} = \frac{\delta\varphi}{\tan \varphi} \tag{14}$$

Figure 2 shows the overall estimated uncertainty in emittance and absorptance as a function of the phase angle for temperatures of 100 and 300 K. The uncertainty in emittance is a minimum for phase angles between 30° and 60° but increases rapidly for smaller or larger phase angles and with decreasing sample temperature. For absorptance measurements, the experimental requirements are not as stringent. The uncertainty in absorptance is independent of temperature and decreases with increasing phase angle, becoming essentially independent of phase angle for angles greater than 45°.

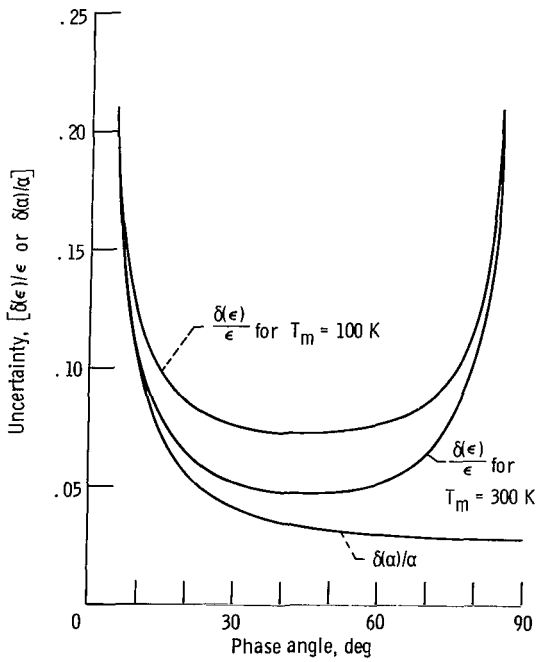

Figure 2. - Absorptance and emittance uncertainty.

Therefore, if only absorptance data are desired, the technique becomes relatively free of experimental difficulties and is ideally suited for absorptance measurements over a large temperature range.

EXPERIMENT

Experimental Requirements

In order to effectively utilize the cyclic technique to provide thermal radiative property data over a range of temperatures, the experiment must be carefully established to satisfy the following primary requirements:

(1) An environment which does not contaminate the sample surface and can be maintained constant for long periods of time without introducing uncontrolled or variable heat-exchange effects between the sample and the environment

(2) A sample mounting arrangement and sample temperature measurement which does not alter the isothermal sample assumption or influence the thermal response of the sample

(3) A variable radiant intensity source which can be varied over a wide intensity range and also precisely controlled over a limited intensity range

Figure 3 illustrates the requirements imposed by the sample response characteristics on an ideal experimental system for a range of temperatures. The two samples considered are 0.001-inch-thick aluminum and 0.001-inch-thick aluminum with both surfaces painted with 3M Black Velvet paint. These two samples illustrate typical sample response characteristics that can be encountered.

For a practical intensity range from 0.01 to 10.0 solar constants (SC), the aluminum sample temperature will vary from 145 to 690 K, while the painted sample will vary from 100 to 600 K. The corresponding time constants for aluminum (based upon c_p values from ref. 10 and emittance values from ref. 11) are 1000 to 8 seconds. For the painted sample (based upon c_p values from ref. 12 and an assumed emittance of unity), the time constants vary from 150 to 2.3 seconds. The time constant is important because it establishes the cyclic frequency required to maintain the proper phase angle and the minimum time required to complete an experiment. The cyclic frequency required to maintain a phase angle of 45° varies from 0.001 radian per second (0.57 rph) at 145 K to 0.045 radian per second (26 rph) at 500 K for the aluminum sample, and from 0.0143 to 0.27 radian per second (8 to 150 rph) for the painted sample at temperatures of 145 and 500 K, respectively. The low cyclic frequencies and long time constants associated with the low sample temperatures require considerable flexibility and long-term stability in the experimental system.

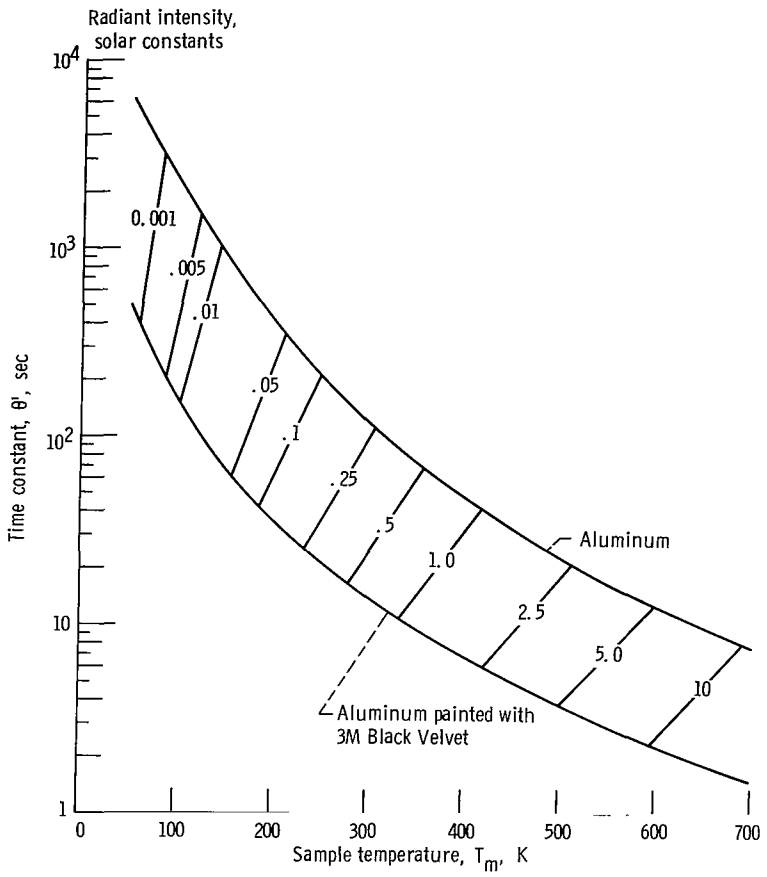

Figure 3. - Response characteristics of 0.001-inch-thick aluminum and 0.001 inch-thick aluminum painted with 3M Black Velvet paint.

Environmental Facility

Figure 4 is a schematic drawing of the experimental facility being used. The test section is cylindrical with a 14-inch diameter and a 10-foot length. The lower 4-foot section of the facility is liquid-helium-cooled to provide cold wall pumping and a 4 K background environment to minimize the background radiant heat load to the samples. The vacuum capability of the liquid-nitrogen cryosorption roughing pumps and the liquid-helium cold wall is below 10^{-10} torr. With such a vacuum, residual gas conduction is negligible. Furthermore, because no oil diffusion or roughing pumps are used, contamination of the sample surfaces by backstreaming of oil cannot occur.

The sample test plane is located deep within the test section with liquid-helium-cooled baffles spaced along the length of the test section to minimize stray radiation from the uncooled upper sections of the facility.

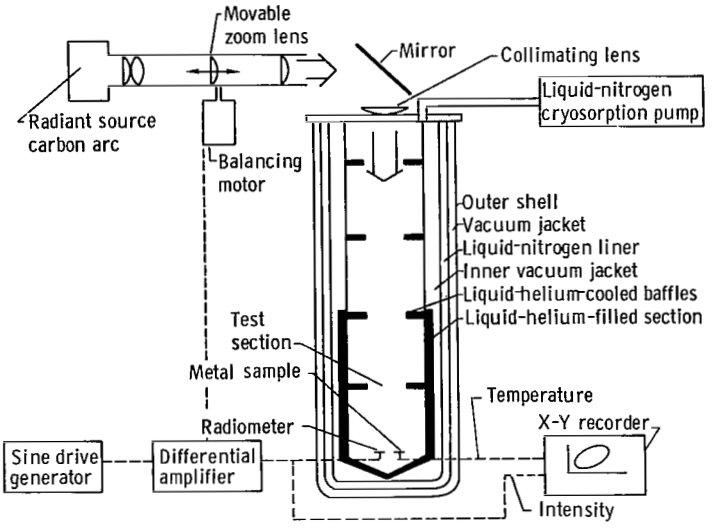

Figure 4. - Schematic drawing of environmental facility.

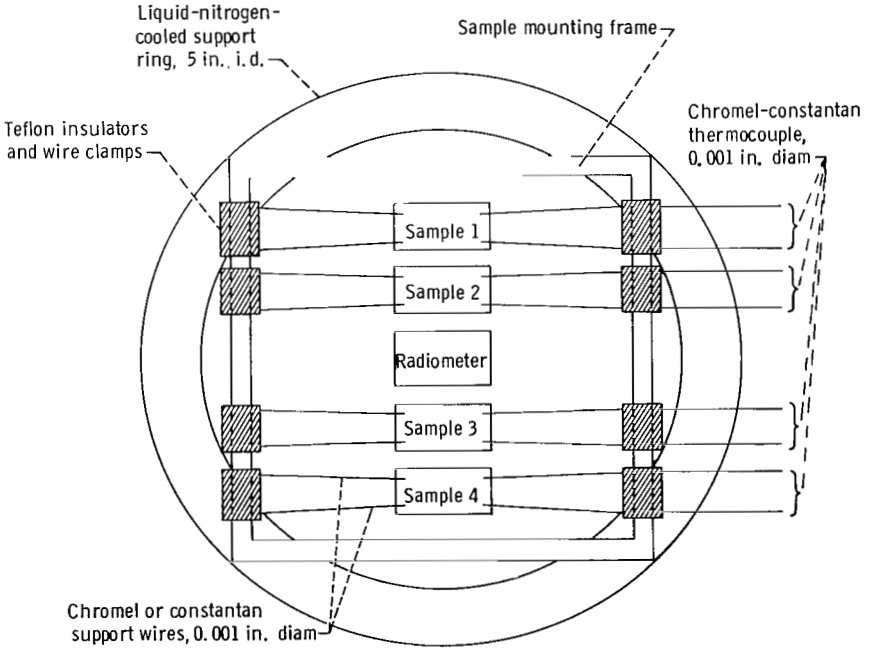

Figure 5. - Schematic layout of sample mounting and thermocouple arrangement.

Sample Mounting

A typical mounting arrangement with four test samples is shown in figure 5. Generally, four samples are installed in order that four sets of complete data may be obtained simultaneously. A radiometer is located in the same test plane at the center of the sample array to monitor the radiant intensity level and to provide feedback control for the sinusoidal intensity variation. The samples are 1 centimeter by 2 centimeters and 0.001 inch thick in order to achieve a fast response time. They are suspended by four 0.001-inch Chromel or constantan wires spot welded to each corner of the samples. Two of the wires are a matched pair Chromel-constantan thermocouple. Chromel or constantan wire, both of which have low thermal conductivities, is used to minimize thermal conduction along the wire. A wire diameter of 0.001 inch is used to minimize thermal conduction and to minimize the effect of the wires on the thermal response of the samples.

Solar Simulator

The solar simulator consists of a 12-kilowatt carbon arc with associated optical elements (fig. 4). The simulator intensity output can be continuously varied by a movable zoom lens over the range from 100 to 250 milliwatts per square centimeter. Lower intensity levels can be obtained by using fine-wire-mesh screens that act as neutral density filters (ref. 13).

The sinusoidal intensity variation is provided by automatic control of the movable zoom lens. The control system is composed of a calibrated silicon solar cell which is coupled with a reference sine generator into a differential amplifier that actuates a balancing motor to maintain the proper position of the zoom lens. The reference sine signal can be varied to produce both the desired amplitude and the cyclic frequency of the sinusoidal perturbation.

The spectral energy distribution of the solar simulator was measured with a double-pass spectrometer that had been calibrated by a transfer method over a wavelength range of 0.25 to 2.5 micrometers. That is, the spectrometer entrance slit was illuminated by a spectrally calibrated 1000-watt, quartz-iodine-tungsten-filament lamp whose calibration was traceable to a National Bureau of Standards (NBS) standard of spectral irradiance. The spectral distribution of the 12-kilowatt carbon arc solar simulator, obtained experimentally (ref. 14), is compared in figure 6 with the solar spectrum (ref. 15). Agreement of the carbon arc curve with the solar spectrum is good over the wavelength region of interest, 0.35 to 2.0 micrometers.

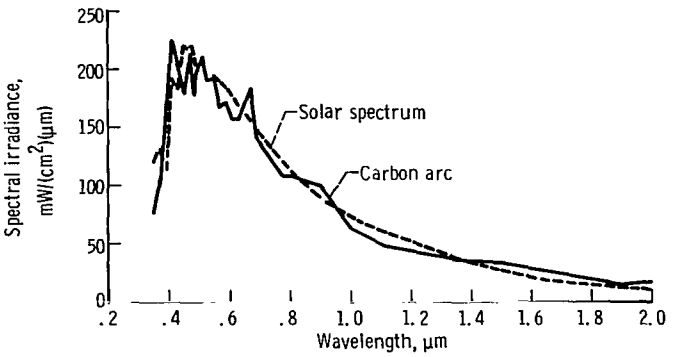

Figure 6. - Spectral irradiance of carbon arc solar simulator.

Procedure

The following procedure was used to obtain data: The radiant intensity was established at an appropriate level and maintained constant until the associated equilibrium sample temperature T_m was reached. After equilibrium was achieved, the intensity was varied sinusoidally at a cyclic frequency and amplitude estimated as that required to provide the proper phase angle and temperature amplitude for accurate data reduction. (The four samples were selected to have compatible response characteristics so that data could be obtained simultaneously at a given cyclic frequency.) The sinusoidal intensity perturbation was continued until cyclic equilibrium was reached as indicated by an unchanging temperature amplitude. Data for phase angle measurements were taken and the data reduced to determine if the phase angle was proper. If the phase angle was not suitable, the cyclic frequency and intensity amplitude were varied accordingly and data again taken at cyclic equilibrium. This procedure was repeated until the proper phase angle and temperature amplitude were obtained.

Measurements

The primary data recorded during the experiment was a Lissajous figure with the intensity on the x-axis and the sample temperature on the y-axis. A typical Lissajous figure is shown in figure 7. To obtain this figure a 0.001-inch-thick stainless-steel-304 sample was exposed to a radiant intensity having a sinusoidal radiant intensity perturbation factor of 0.2 and cyclic frequency of 6 rph. The Lissajous figure provides all the necessary data on a single figure. The mean radiant intensity, intensity amplitude factor, mean temperature, and temperature amplitude are all accurately recorded with

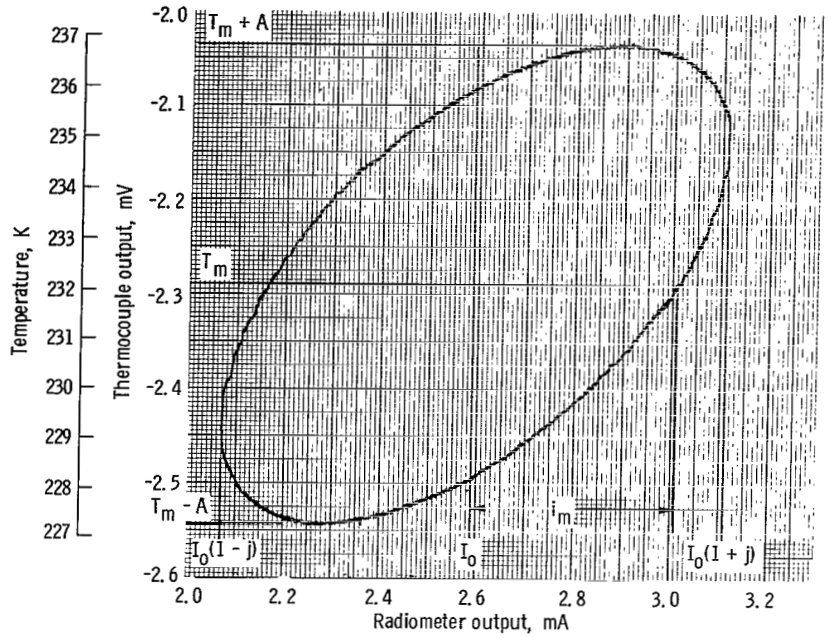

Figure 7. - Typical Lissajous figure for 0.001-inch-thick stainless-steel-304 sample. Cyclic frequency, 6 revolutions per hour; mean intensity, 2.59 milliamperes; intensity amplitude factor, 0.2.

good resolution. The phase angle measurements are determined from the figure by (ref. 16)

$$\tan \varphi = \left[\left(\frac{jI_o}{i_m} \right)^2 - 1 \right]^{-1/2} \tag{15}$$

and

$$\sin \varphi = \frac{i_m}{jI_o} \tag{16}$$

The Lissajous figure also provides a useful monitoring function over the experiment in that the figure must close and repeat when cyclic equilibrium is achieved.

Accuracy

The accuracy of the emittance and absorptance determination can be estimated by

considering the uncertainty in the various required parameters that are determined from the Lissajous figures. The intensity and temperature level can be resolved quite accurately. Any errors involved in these parameters are due to the calibration of the radiometer and the sample thermocouple. The uncertainty is within 0.01 for the radiometer, and the uncertainty interval is within 2 K for the thermocouple.

The uncertainties in $\tan \varphi$ and $\sin \varphi$ are determined from

$$\frac{\delta \tan \varphi}{\tan \varphi} = (1 + \tan^2 \varphi) \left[\left(\frac{\delta j I_o}{j I_o} \right)^2 + \left(\frac{\delta i_m}{i_m} \right)^2 \right]^{1/2} \tag{17}$$

and

$$\frac{\delta \sin \varphi}{\sin \varphi} = \left[\left(\frac{\delta j I_o}{j I_o} \right)^2 + \left(\frac{\delta i_m}{i_m} \right)^2 \right]^{1/2} \tag{18}$$

The uncertainty in the intensity amplitude factors is estimated to be $\delta j I_o / j I_o = 0.01$ and $\delta i_m / i_m = 0.02$ for phase angles greater than 40^o. For phase angles less than 40^o, the uncertainty in $\delta i_m / i_m$ increases, while that for $\delta j I_o / j I_o$ remains constant. The uncertainty in the specific heat for stainless steel 304 is estimated to be 0.05, while the uncertainty for a pure metal is estimated to be 0.02. Based upon these values, the uncertainties in emittance and absorptance as given by equations (11) and (12) are $\delta \epsilon / \epsilon \approx 0.09$ and $\delta \alpha / \alpha \approx 0.06$ for the stainless-steel-304 sample. However, had the sample been a pure metal, the uncertainties would have been $\delta \epsilon / \epsilon \approx 0.07$ and $\delta \alpha / \alpha \approx 0.04$ because of the better estimate of the specific heat.

In addition to the uncertainties which can be estimated, there are sources of error present that must be recognized and considered but whose effect cannot be estimated. Examples of these are nonuniformities in the radiant beam across the test plane and radiation bounce-back from the bottom of the tank to the samples. The uniformity of the beam has been evaluated in reference 14 and found to be within ±2 percent. The bottom and sides of the test facility have been painted black ($\alpha \approx 1.0$), and apertures are used to minimize the bounce-back.

Other possible sources of error are physical nonuniformity of the sample surface, contamination of the sample surface, and the spectral match of the solar simulator to the solar spectrum. These effects introduce systematic uncertainties into the radiative properties of the sample, and as a result, the radiative properties are only representative for the source and the sample used.

RESULTS AND DISCUSSION

Experimental Evaluation of Technique

If the perturbation technique is to measure the total hemispherical emittance and normal solar absorptance accurately, the following requirements must be satisfied:

(1) The phase angle, as determined from the Lissajous figure, should accurately represent the experimental system at thermal equilibrium.

(2) Tan φ against ω (eq. (5)) and A against $(jI_o/\omega) \sin \varphi$ (eq. (7)) should be linear relations for a constant sample temperature.

(3) The heat-loss term q should be constant.

(4) The associated radiation source should have good uniformity and very good stability to ensure cyclic equilibrium at the lower sample temperatures. Since these properties of the cyclic method are unknown, it was necessary to evaluate each of them under laboratory conditions to ascertain the validity of the cyclic radiation method for determining thermal radiative properties.

In order to test the first property, a 1-kilowatt quartz-iodine-tungsten-filament lamp was used as a radiation source because of its very good stability over long periods of time. Its radiant intensity level was established to provide a sample temperature of approximately 260 K. After this temperature level was established, the radiant intensity was cycled at 4 rph with an intensity amplitude j of approximately 0.565. The resulting Lissajous figure obtained for a 0.001-inch-thick molybdenum sample is shown in figure 8. This figure was then analyzed and a phase angle φ determined. With this value for φ, a Lissajous figure was calculated and is shown as the dashed curve in figure 8. Note that the agreement between the experimentally obtained Lissajous figure and the calculated figure is not exact over the complete cycle but the agreement is good and no asymmetries are evident in the experimental curve. The following observations can now be made:

(1) Cyclic equilibrium was obtained since the figure closed and was repeatable.

(2) The phase angle determined from one cycle accurately described the experimental conditions over one complete cycle.

(3) The temperature response was truly sinusoidal. Thus, the linearized analytic solution is valid for the conditions of this particular experiment.

(4) The resulting Lissajous figure has adequate resolution for an accurate determination of the pertinent parameters T_m, A, I_o, i_m, and jI_o.

Equations (6) and (7) reveal that $\tan \varphi$ and A must vary linearly with ω and $(jI_o/\omega)\sin \varphi$, respectively, for the cyclic method to be valid. Experiments were conducted for cyclic frequencies varying from 2 to 30 rph, and intensity amplitude ratios ranging from 0.0768 to 0.565. These data are shown in figures 9 and 10 for 0.001-inch

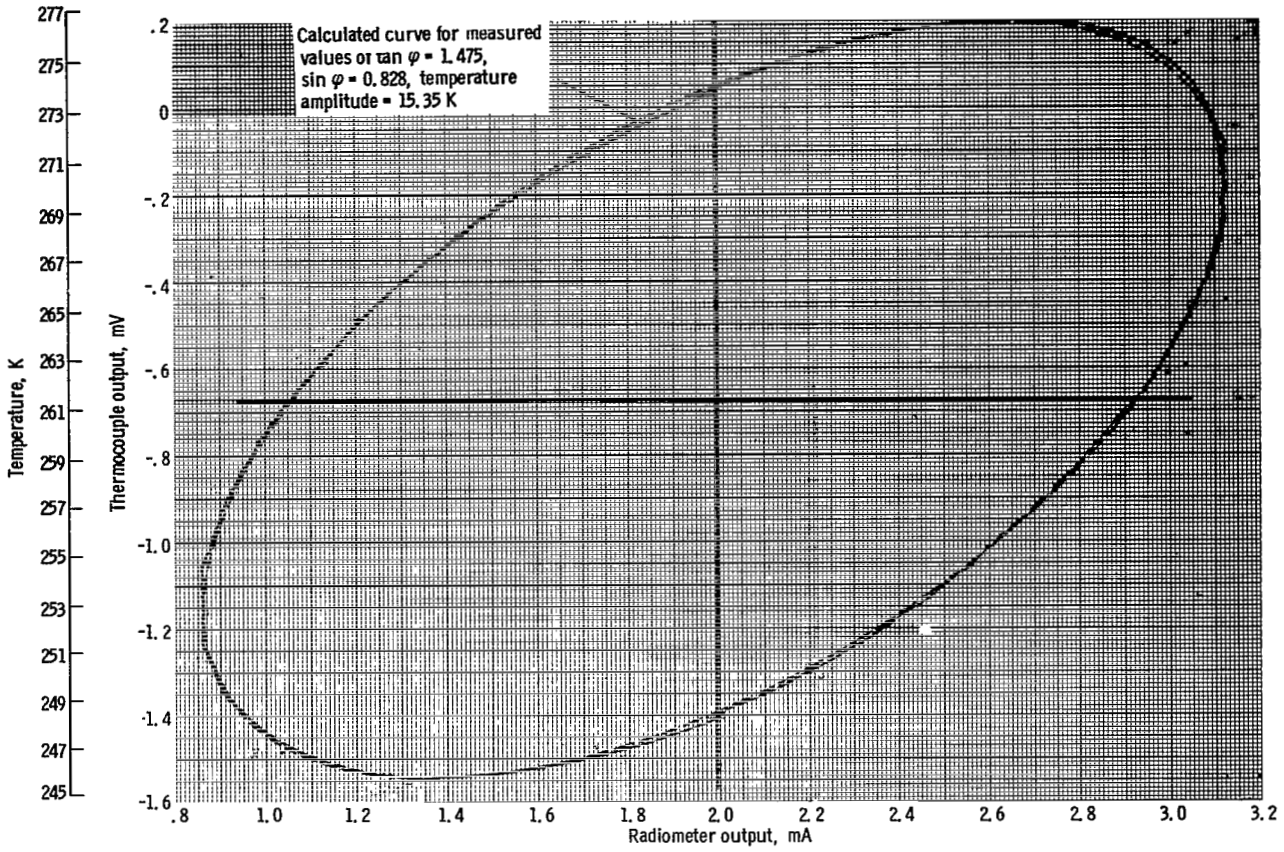

Figure 8. - Experimental and calculated Lissajous figures. Sample, 0.001-inch-thick molybdenum; cyclic frequency, 4 revolutions per hour; mean intensity, 1.99 milliamperes; intensity amplitude, 1.13 milliamperes.

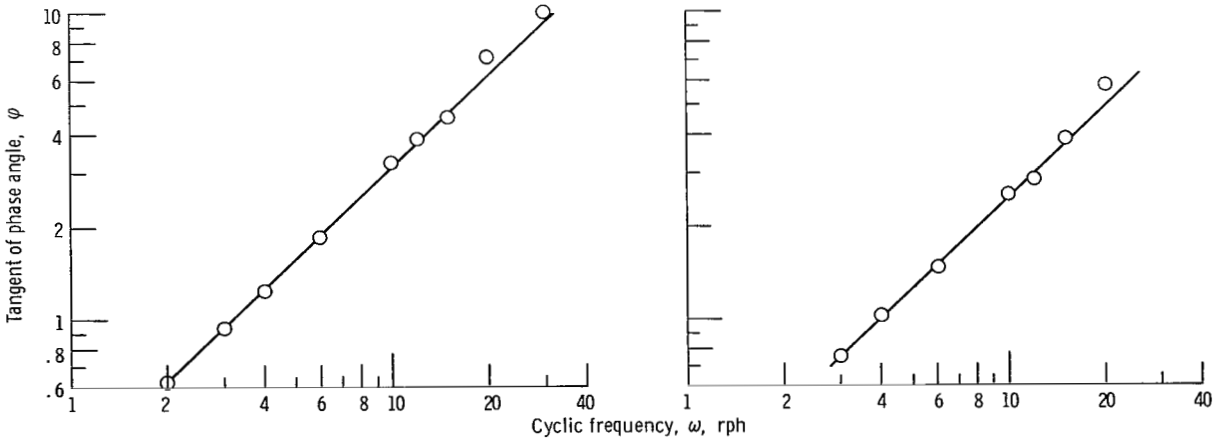

(a) Sample, 0.001-inch-thick molybdenum. Mean sample temperature, 275 K.

(b) Sample, 0.005-inch-thick molybdenum painted with 3M Black Velvet paint. Mean sample temperature, 180 K.

Figure 9. - Variation of phase angle with cyclic frequency.

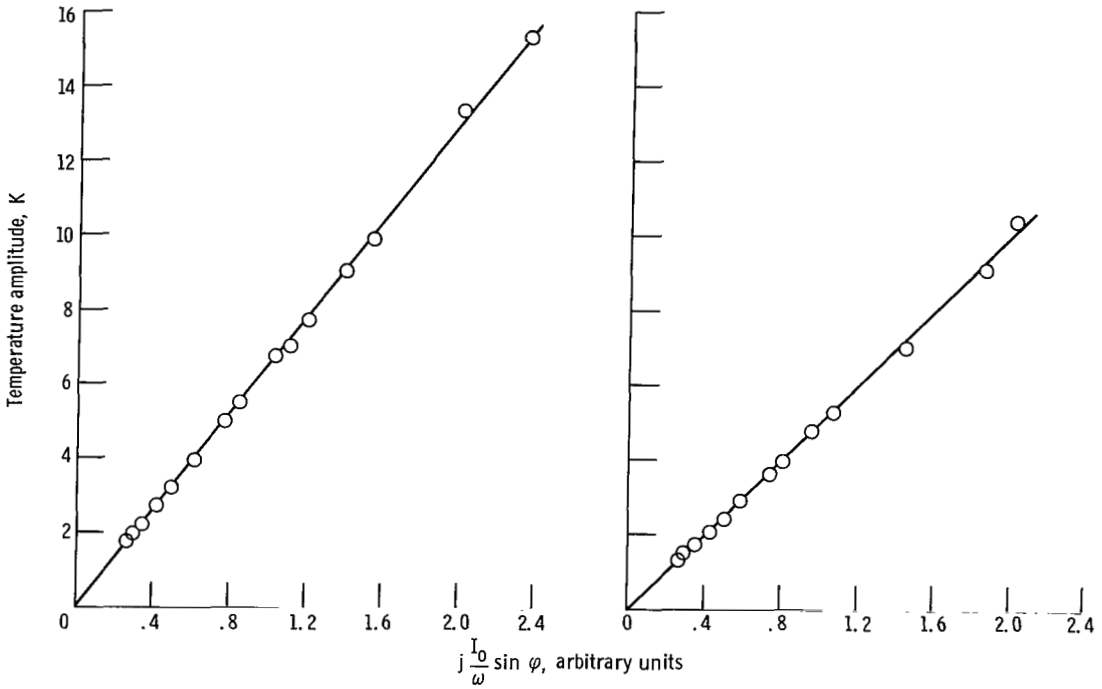

(a) Sample, 0.001-inch-thick molybdenum. Mean sample temperature, 275 K.

(b) Sample, 0.005-inch-thick molybdenum painted with 3m Black Velvet paint. Mean sample temperature, 180 K.

Figure 10. - Variation of temperature amplitude with cyclic frequency and intensity amplitude. Mean temperature held constant.

molybdenum and for 0.005-inch molybdenum painted with 3M Black Velvet. For every sample temperature, the data vary linearly for the materials used. Thus, this series of experiments demonstrates conclusively that the analysis, or the technique, is valid over a wide range of operating conditions.

Although the analysis has been conclusively demonstrated to be proper, it remains to be proven that the emittance and absorptance determined are the true values. In particular, the correctness of the emittance determination is directly related to the constancy of the heat-loss term q, as indicated in the theoretical section. If q varies slightly from a constant value, as would be expected for a temperature perturbation (e.g., conduction losses), the true sample emittance as given previously by equation (10) is

$$\epsilon_{meas} = \epsilon_{true} \mp \frac{K}{8\sigma A_s T_m^3} \tag{10}$$

The effect of the variation of q with temperature on the measured emittance can be de-

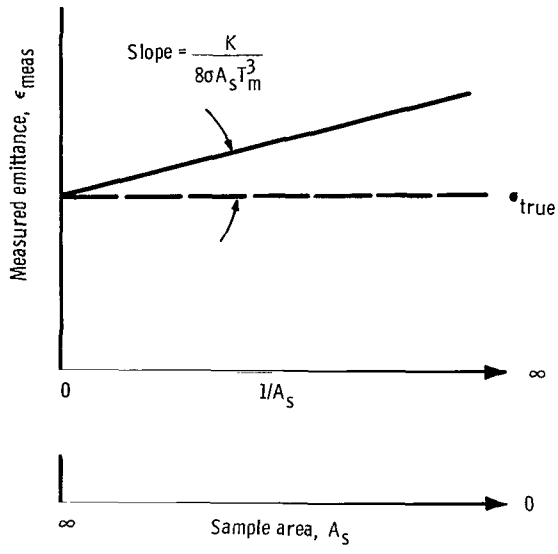

Figure 11. - Variation of measured emittance with sample area.

termined from a series of tests wherein the sample area A_s is the only parameter varied. With such data a plot of ϵ_{meas} against the reciprocal of sample area is linear, and in particular, the intercept of such a plot is the true emittance, as shown in figure 11. Such a series of tests were run at several temperatures, and the data obtained are presented in figure 12. The following observations can be made:

(1) The measured emittance is related linearly to the reciprocal of the sample area as indicated by the analysis.

(2) The slope of the straight line variation decreases as the mean temperature increases. Thus, the measured emittance and the true emittance are approximately equal at the higher temperatures.

(3) At the lower temperatures, the true emittance and the measured emittance are different; therefore, a sample area as large as possible should be used. The maximum area usable is dictated, of course, by the uniformity of the radiation source (or the uniformity of the sample temperature) since the sample must be isothermal for the analysis to be valid.

It was stated previously in the theoretical section that the absorptance, as determined by the cyclic technique, was unaffected by a heat-loss mechanism. In order to test this conclusion, the absorptance (or its equivalent, $A/j \sin \varphi$) was also determined from the same series of tests used for figure 12(a). These data are plotted in figure 12(b) with the reciprocal of the sample area as the independent variable. Each curve presented is for constant temperature, intensity and cyclic frequency. Therefore, the parameter $A/j \sin \varphi$ is directly proportional to the absorptance. For every tem-

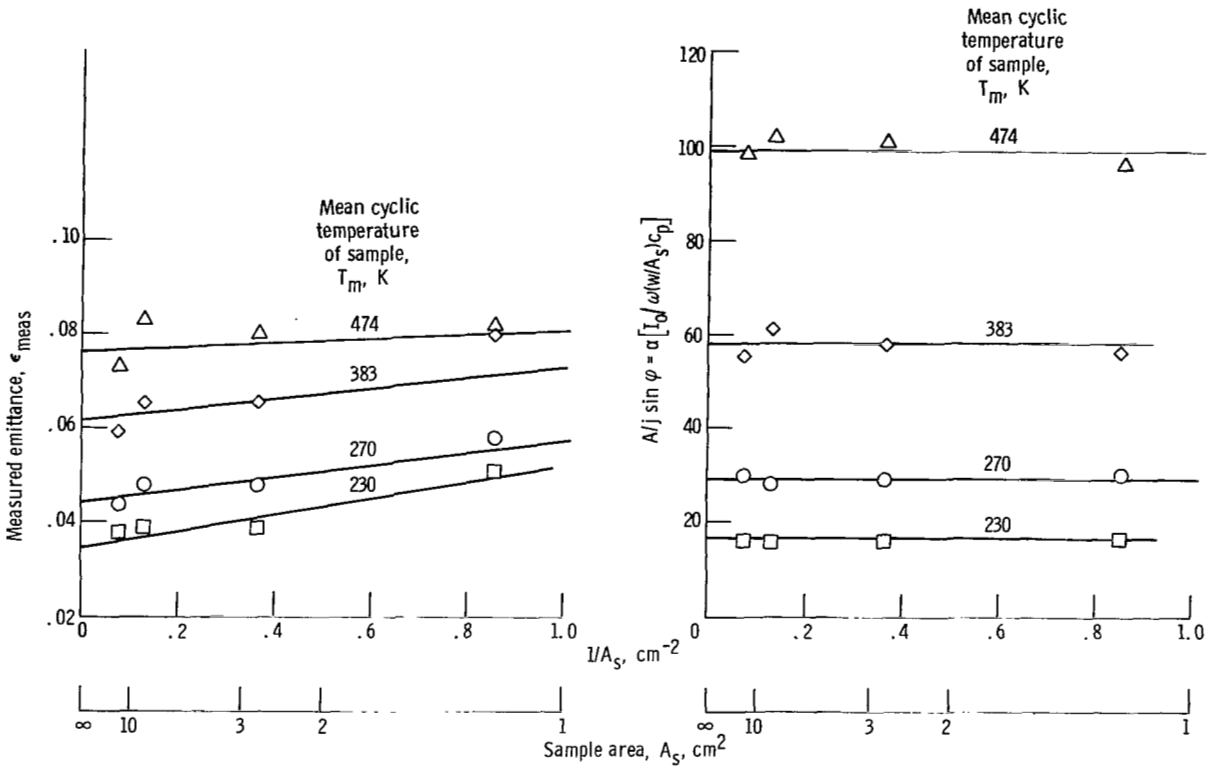

Figure 12. - Effect of sample area on measured parameters.

perature, the absorptance is independent of the sample area and thus is independent of any heat-loss effect.

Radiation source stability is a must since the material time constant increases rapidly as the sample temperature decreases. In general, the time to achieve cyclic equilibrium is at least five times the material time constant. For example, a copper sample investigated at 162 K had a time constant of 1046 seconds. Thus, with a cyclic frequency of 0.0042 radian per second (2.4 rph), absolute control of the radiant intensity was required for a period in excess of 2 hours to obtain a Lissajous figure that not only closed but also repeated itself. Time constants of this order do not represent a difficult experimental problem. However, for temperatures less than approximately 150 K where the time required to reach equilibrium is greater than 2 hours, minor intensity disturbances (or temperature disturbances) during a cyclic period can result in system perturbations which may require a restart of the test.

Two methods have been used to minimize this problem. The time constant of a given material can be substantially reduced by depositing a thin layer of the material under investigation upon a metal substrate having a more suitable time constant. For example, molybdenum and lead can be used effectively because of their small time constants. If only emittance data are required, a tungsten-filament lamp, which is a very stable source, can be used at lower temperatures.

As a final check on the validity of the cyclic radiation technique, the solar absorptance of various materials was obtained from spectral reflectance data obtained with a double-pass monochromator and an 8-inch-diameter magnesium-oxide-coated integrating sphere. The integrating sphere method is a generally accepted method for determining solar absorptance. The data obtained by using an integrating sphere are compared with those obtained with the cyclic technique in the following section. In general, the agreement between the data is very good for the materials chosen and the temperature range covered.

Although the data presented to establish the validity of the cyclic radiation technique for determining thermal radiative properties is not positively conclusive, the authors feel it is sufficient. As will be indicated herein, both accurate emittance and absorptance data can be obtained over a large temperature range for various materials, including metals, coatings, and composites. In addition, the technique possesses a degree of versatility and convenience that no other method offers.

Thermal Radiative Properties

Metals. - The thermal radiative properties ϵ, α, α/ϵ of 12 metals (aluminum, copper, gold, molybdenum, nickel, platinum, silver, 304 stainless steel, tantalum, tin, titanium, and vanadium) were obtained. These data are shown in figure 13 for temperatures ranging from approximately 200 to 560 K. In general, the total hemispherical emittance of the metals increased with increasing temperature, the normal solar absorptances were approximately constant, and the absorptance-emittance ratio decreased with increasing temperature because of the increase in emittance.

In addition to the solar absorptance data obtained in the space environmental facility with the carbon arc solar simulator, solar absorptance data on the same metals were determined from spectral reflectance data obtained from integrating sphere measurements (ref. 8). The comparison between the measured carbon arc solar absorptance and the solar absorptance obtained from the integrating sphere reflectance measurements are shown in figure 13. For all the metals, the agreement between the absorptance values is good.

Comparison of metal data with theory. - There are three basic theories with which to conveniently compare experimentally determined total hemispherical emittance: (1) the Hagen-Rubens relation (HR), (2) the Drude single electron theory (DSE), and (3) the anomalous skin effect theory (ASE). A comparison of these theories with experiment is made in an effort to assess their suitability for making predictions of thermal radiative properties and to gain further insight into the validity of the cyclic technique.

Each of the theories is based on the solutions of Maxwell's equation, which establish the correspondence between the optical parameters, refractive index n and extinction

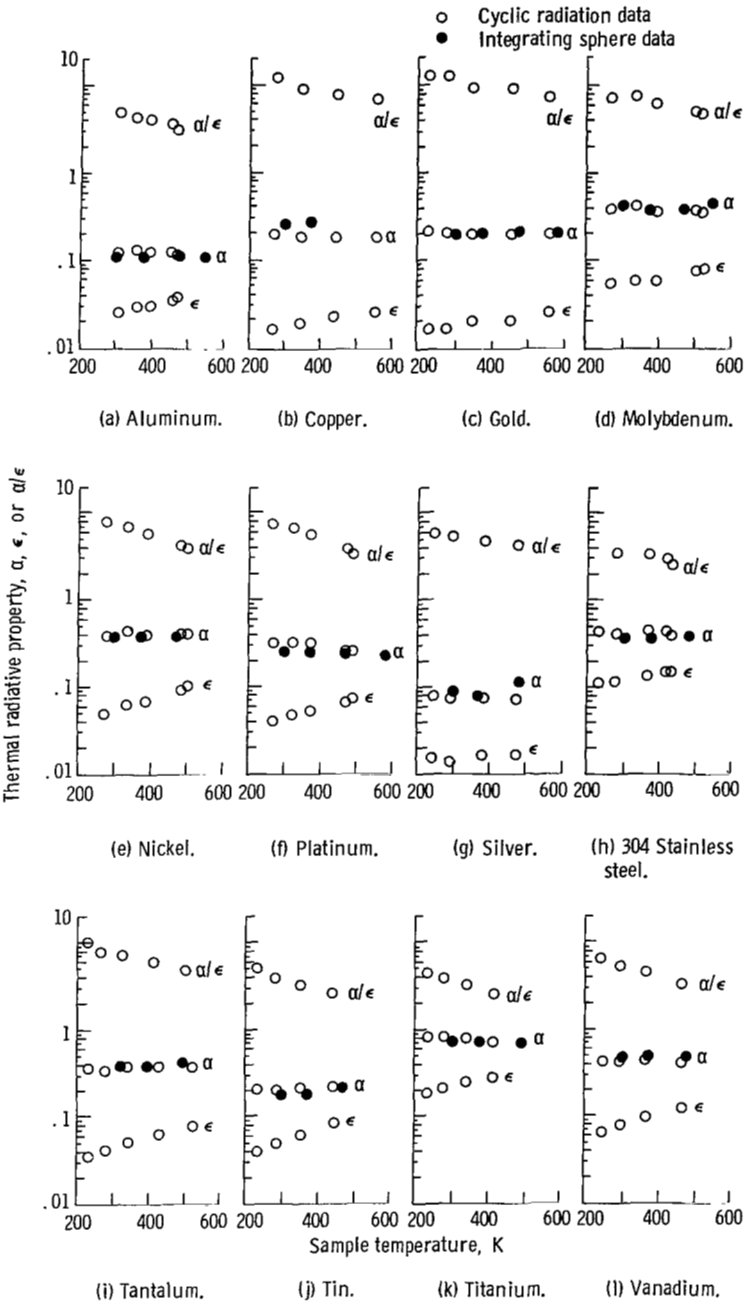

Figure 13. - Radiation property data of metals.

coefficient k, and the electric and magnetic properties of a material. From the Fresnel equation for reflectance, the spectral normal emittance in terms of the optical parameters is

$$\epsilon_n(\lambda) = \frac{4n}{(n+1)^2 + k^2} \tag{19}$$

The total normal emittance is then determined by the integration of the product of the spectral emittance and the Planck spectral energy distribution over all wavelengths. Finally, the total hemispherical emittance for metals is determined from the total normal emittance by (ref. 17)

$$\epsilon = 1.33\,\epsilon_n \tag{20}$$

A detailed discussion of the basic theories and their application to total emittance calculations is presented in references 18 and 19.

The total hemispherical emittance data obtained experimentally for all the metals are compared in figure 14 with the analytical relation derived from the Hagen-Rubens spectral emittance. The Hagen-Rubens equation for the total hemispherical emittance is (ref. 18)

$$\epsilon \approx 0.766\left(\frac{T}{\sigma_e}\right)^{1/2} \tag{21}$$

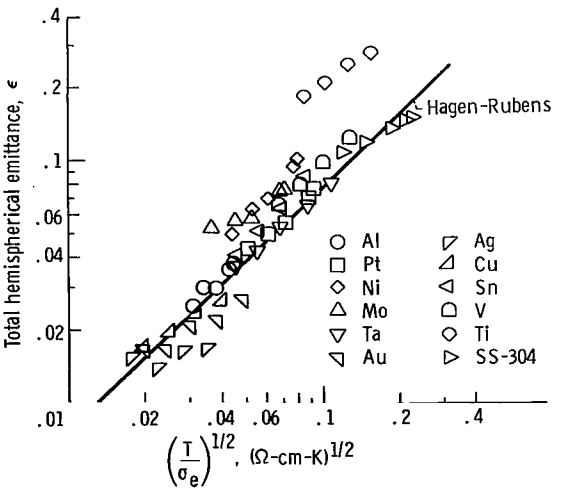

Figure 14. - Comparison of all experimental data with Hagen-Rubens equation.

The Hagen-Rubens equation correlates the absolute level of the total hemispherical emittance data for all the metals except titanium to within ±50 percent. However, it should be recognized that titanium is a very active metal so that surface contamination is probably the cause of the large disagreement noted for this metal. (The values used for direct-current electrical conductivity in equation (21) were obtained from refs. 10 and 11 except for tin and 304 stainless steel, which were obtained from ref. 20.) For many engineering purposes, the comparison shown in figure 14 is both quantitatively and qualitatively acceptable. The fact that the theory does correlate the data for the 12 different metals with modest success probably indicates that the direct-current electrical conductivity of the metal represents the effective conductivity of most metals regardless of the atomic structure and the small amount of surface contamination present. The comparison, however, leaves much room for improvement if very accurate thermal emittance data are required. In that case, experimental data on the particular material are needed.

The experimental data for four metals are compared with the Hagen-Rubens, DSE, and ASE theories in figure 15. The metals chosen are the noble metals copper, gold, and silver and the nonnoble metal aluminum. The noble metals were chosen because of their compatability with the assumption of a single free conduction electron in the DSE and ASE theories (ref. 21). Aluminum was chosen because of its general application in many areas of space technology.

Several observations can be made from the comparisons in figure 15. The Hagen-

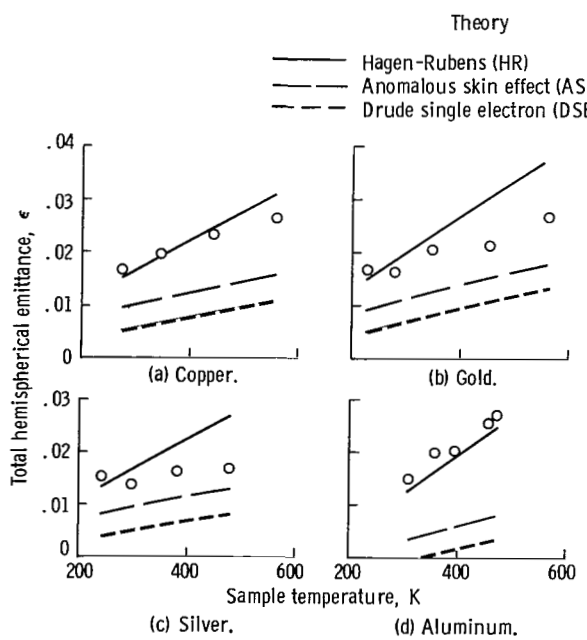

Figure 15. - Comparison of experimental data with theory.

Rubens theory predicts the absolute level of the emittance for copper and aluminum with fair accuracy but only approximately for gold and silver. The Hagen-Rubens prediction agrees more closely with the experimental data as the temperature approaches 250 K. Both the ASE and DSE theories predict emittance values which are lower than the experimental data. The variation of emittance with temperature for aluminum is predicted well by the Hagen-Rubens relation, while the ASE and DSE theories predict the slope much better for the noble metals.

Although the DSE and ASE theories are considered more rigorous than the HR theory, the quantitative agreement with experimental data is not as good. However, this disagreement must be viewed in light of the assumptions made in deriving the electromagnetic theories. All the theories assume an ideal interaction between the incident electromagnetic waves and the material surface. Physically this means, for example, that the surface is optically smooth and uncontaminated. The fact that ideal surfaces do not exist in experiments is probably responsible for the differences noted between theory and experimental data. Thus, such factors as impurities, contamination, surface finish, and crystal structure can significantly affect the actual thermal radiative properties. Such nonideal surface effects tend to increase the emittance of metals. For temperatures greater than approximately 200 K, the HR approximation yields results higher than those of the more exact theories. Therefore, the HR relation frequently correlates the experimental data better than the more exact theories. This improved agreement is therefore probably fortuitous, but it is representative of results obtained with real materials.

In summary, all the metal data obtained by the cyclic technique have indicated the following conclusions: When compared with theory, the level of the data is proper, and in particular, the trend of the data with temperature is proper. In addition, the absorptance data obtained for 12 metals by utilizing the cyclic technique is in good agreement with data obtained from spectral reflectance measurements made using an integrating sphere. These results indicate that the cyclic method of determining thermal radiative properties is a valid one.

Composite - CdS solar cell. - The optical properties of a composite material, namely a CdS solar cell, were obtained at temperatures corresponding to radiant intensities that varied from 0.04 to 1.1 SC. The time constants (eq. (5c) as determined from the measured phase angle φ and imposed frequency ω are shown in figure 16. It is to be noted that the response time increases with decreasing temperature, and that the longest time constant obtained is 143 seconds at a cell temperature of 156 K. Therefore, the longest time required to reach cyclic equilibrium is of the order of 12 minutes. Since this time is relatively short, there are no difficulties in meeting the critical requirement that all experimental parameters be held constant for this period.

Two data points obtained with the 1-kilowatt quarts-iodine-tungsten-filament bulb

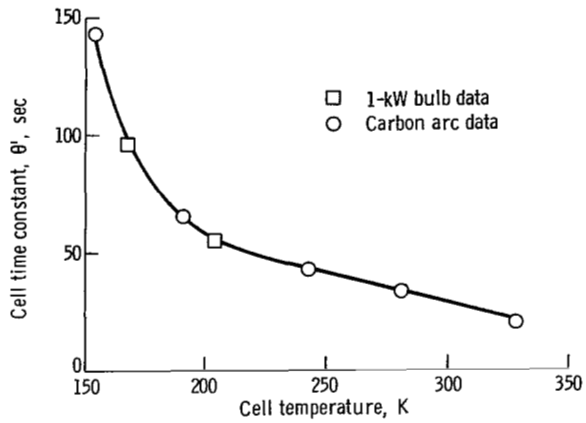

Figure 16. - Time constant of cadmium sulfide solar cell.

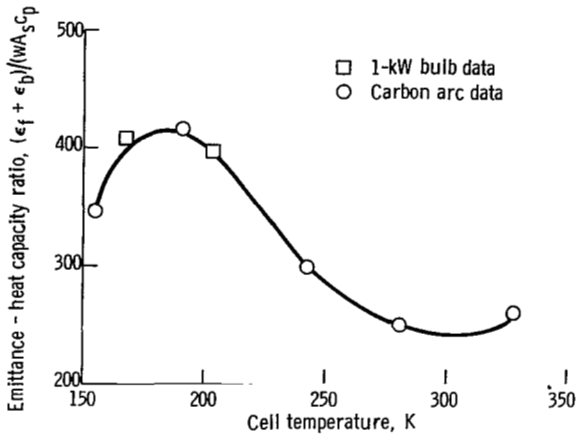

Figure 17. - Emittance of cadmium sulfide solar cell.

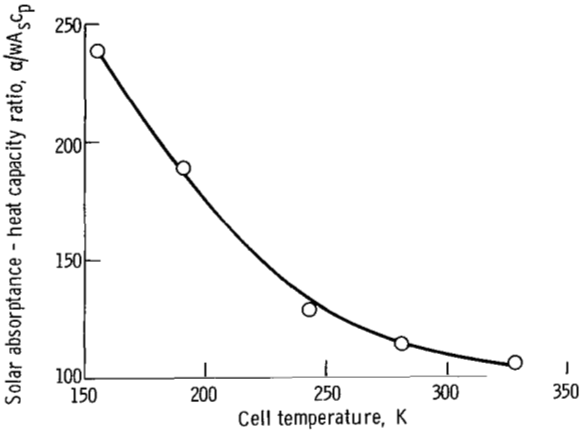

Figure 18. - Solar absorptance of cadmium sulfide solar cell (carbon arc source).

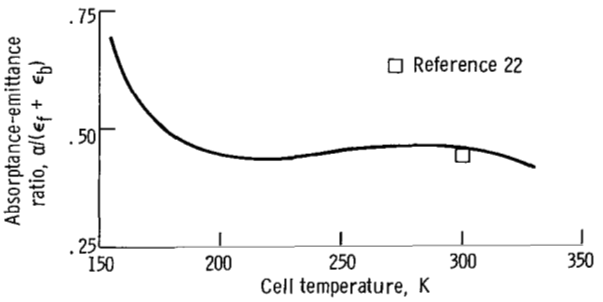

Figure 19. - Absorptance-emittance ratio for cadmium sulfide solar cell.

are also included in figure 16 since the cell time constant is unaffected by the source spectral distribution. Data from the 1-kilowatt bulb are much more accurate than those obtained with the arc lamp because there are no instability problems. Despite this, however, all the time constants are very consistent regardless of the source used.

With the time constant established, the emittance can be determined (eq. (6)) from the same data points. Again, data from both sources can be used to obtain emittance. Solar absorptances are obtained by substituting in equation (7) the additional measurements of temperature amplitude A and intensity amplitude jI_o. In this case, however, the 1-kilowatt-bulb data cannot be used since its spectral distribution is not comparable to the solar spectrum.

The emittance and absorptance data obtained are presented in figures 17 and 18 in terms of the cell heat capacity per unit area. Unfortunately, this had to be done because no specific-heat data are available for CdS solar cells. As a result, the character of these plots is influenced greatly by the cell specific heat variation with temperature.

Even so, the plots could be utilized to obtain absorptance and emittance by those who are willing to estimate the specific heat of the solar-cell materials.

The important optical parameter, the parameter establishing the cells operating temperature, is the absorptance-emittance ratio. This parameter can readily be obtained, without any assumptions, by ratioing the curves presented in figures 17 and 18. The absorptance-emittance ratio is shown in figure 19 for cell temperatures ranging from approximately 150 to 325 K. The important trend to note is the rapid increase in the absorptance-emittance ratio as the temperature is decreased. As the temperature increases from 155 to about 200 K, the absorptance-emittance ratio decreases from 0.70 to about 0.43, a decrease of 39 percent. A further increase in temperature produces little change; the α/ϵ ratio is approximately constant at a value of 0.43 from 200 to 325 K. Comparison of the 300 K experimental point presented in reference 22 with the preceding data shows good agreement. As a point of information, it should be noted that the cell was not producing power when the optical properties were obtained. As a result, the temperatures measured are slightly high. Calculations indicate that, for a cell having an electrical conversion efficiency of 5 percent, the equilibrium cell temperature, while producing power, may be as much as 6 K lower than that presented herein.

Paints and coatings. - Currently underway at Lewis is a program to determine the thermal radiative properties of various thermal control paints and coatings using the cyclic radiation technique. The cyclic technique can be used readily if the coating (or paint) can be properly applied to a suitable substrate and if the specific heat of the paint or coating is known. This latter requirement presents a difficulty since the specific heats of paints and coatings are not generally available. Fortunately, however, the cyclic technique can be used in several ways to determine the specific heats of paints and coatings, so that thermal radiative properties can be determined. To illustrate the use of the cyclic technique for coatings and paints, data were obtained for 3M Black Velvet paint and for the Z-93 white coating. The specific heat for Z-93, which was unknown, was also determined in this experiment. These data, along with the solar absorptance data obtained at 300 K by integrating sphere reflectance measurements, are presented in figure 20.

3M Black Velvet paint: The 3M Black Velvet paint sample consisted of a 0.005-inch-thick molybdenum substrate upon which the paint was applied to both surfaces. The paint weight was approximately 8 percent of the substrate weight. The specific heat of the paint was obtained from reference 12. The radiative property data indicate that the emittance and absorptance are approximately equal and are greater than 0.95 over the temperature range from 180 to 315 K. The comparison of the absorptance determined by the cyclic method with the integrating sphere reflectance measurement ($\alpha = 0.97$) at a temperature of 300 K is good. The measured cyclic absorptance of 1.06 at 315 K is, of course, too high. This value, however, is within the accuracy of the method and indicates that the solar absorptance of the 3M Black Velvet paint is very nearly unity.

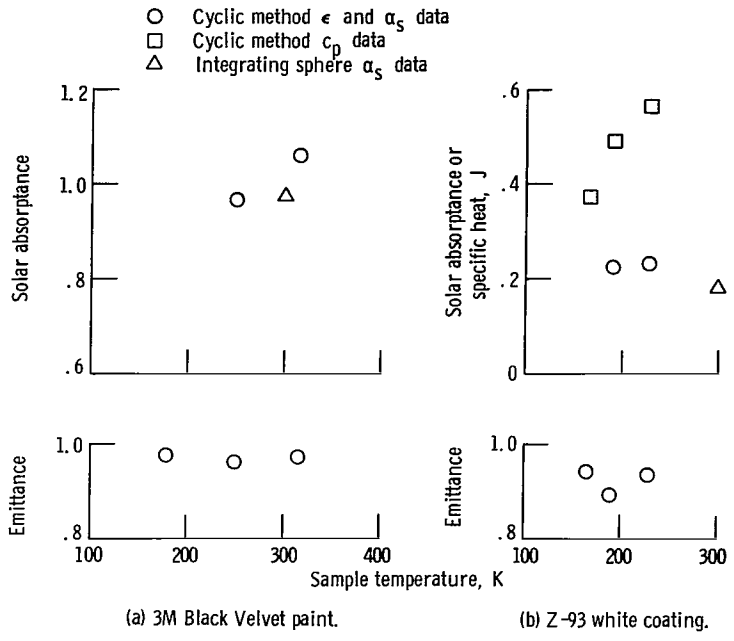

(a) 3M Black Velvet paint. (b) Z-93 white coating.

Figure 20. - Absorptance and emittance of 3M Black Velvet paint Z-93 white coating.

Z-93 white coating: The method chosen initially to determine the Z-93 white coating specific heat was as follows. The coating was applied to both surfaces of two different substrate materials. The substrate materials selected were 0.005-inch-thick nickel and molybdenum and were chosen because of their different thermal response characteristics. The specific heat of the coating was determined by a simultaneous solution of the measured sample time constants for a given temperature and for an assumed equal coating emittance on the samples by

$$\left(c_p\right)_c = \frac{\frac{w_2}{\left(A_s\right)_2}\left(c_p\right)_2 \theta_1' - \frac{w_1}{\left(A_s\right)_1}\left(c_p\right)_1 \theta_2'}{\frac{\left(w_c\right)_1}{\left(A_s\right)_1}\theta_2' - \frac{\left(w_c\right)_2}{\left(A_s\right)_2}\theta_1'} \tag{22}$$

The data in figure 20 show the emittance of the Z-93 coating to be approximately 0.92 and the absorptance to be 0.23 over the temperature range from 165 to 230 K. The comparison between the absorptance data from the cyclic technique (which is the average of the two samples) and the integrating sphere reflectance measurements at a temperature of 300 K (α = 0.18) was not as good as expected. The differences noted here are

attributed to differences between the arc lamp spectral distribution and the solar spectrum (ref. 14), errors in the wavelength limitations of the integrating sphere instrumentation (see ref. 8), and the error in the specific-heat determination.

The determination of the coating specific heat is another illustration of the versatility and usefulness of the cyclic technique. However, it should be noted that the procedure of using two different substrates to determine specific heat is not the only procedure that can be used. In fact, it probably is not the best procedure because the assumption of equal coating emittance of the two samples is subject to question. A more suitable approach is to coat the back side of a pure metal standard whose absorptance is known and expose it to a known cyclic radiation. The coating specific heat can then be determined from

$$\left(c_p\right)_c = \frac{\alpha_s A_s j I_o \sin \varphi}{w_c \omega A} - \frac{w_s \left(c_p\right)_s}{w_c} \tag{23}$$

where α_s is the solar absorptance of the metal standard. Thus, the coating specific heat can be determined in terms of the absorptance of a pure metal, which for most metals is independent of temperature.

CONCLUDING REMARKS

Considerable experience has been gained in the application of the cyclic radiation technique to determine thermal radiative property data for various materials. The primary advantages of the method are

1. The emittance and absorptance are determined simultaneously.

2. Radiative property data can be obtained conveniently for many different types of materials over the temperature range from 150 to 600 K.

3. The technique is not affected by the magnitude of any extraneous heat-loss effects. The variation of the heat loss over the range of the temperature perturbation does not affect the absorptance determination but can introduce a slight effect into the emittance determination. The error in emittance, however, is much less than that encountered by other methods, which must account for the magnitude of the heat loss.

4. There is versatility in the technique since the experimental parameters, cyclic frequency and intensity level, can be controlled to yield accurate data irrespective of the temperature level and the magnitude of the material radiation properties.

5. The specific heat of coatings and paints may be determined by using a suitable metal standard for a substrate.

The cyclic method is fairly convenient to apply but there are certain experimental requirements that must be met, as follows:

1. The sample configuration is governed by the requirements of the technique. The sample must be a thin, flat section for reasonable response time, and the sample must have an exposed area of at least 2 square centimeters.

2. The sample material (or the substrate) must be suitable for attaching small-diameter support and thermocouple wires.

3. The specific heat of the sample material (and substrate) must be accurately known.

4. A versatile radiation source must be available which can be precisely controlled in a sinusoidal manner. In addition, the amplitude and cyclic frequency of the sinusoidal variation must be variable over a large range and capable of being maintained constant for long periods of time.

Considerable data have been obtained to check the validity of the method and no serious problem areas have arisen. The method has generally provided very consistent data over a large range of operating conditions and experimental variables. The primary requirement for obtaining accurate data is to maintain the phase angle between 40° and 60°. This is conveniently accomplished by adjusting the incident radiation cyclic frequency.

The most serious limitation of the method is considered to be the fairly long response times encountered for some materials, during which absolute control over the experiment must be maintained. Therefore, thin samples having the desired fast response times are preferred and, in general, have been used.

Thermal radiative property data were obtained for a variety of materials at temperatures ranging from 150 to 600 K. The following summary remarks can be made.

The total hemispherical emittances and solar absorptances obtained for 12 metals are consistent and follow the accepted variation with temperature. No comparison can be made regarding the level of the emittance obtained except that the results appear to be reasonable when compared to theory and other available experimental data. The comparison between the cyclic solar absorptances and those obtained from integrating sphere reflectance measurements is good.

A composite, namely a thin film CdS solar cell, was investigated over temperatures ranging from 155 to 325 K. The absorptance-emittance ratio $\alpha/(\epsilon_f + \epsilon_b)$ of the cell was approximately constant over the temperature range 200 to 325 K. Below 200 K the ratio increased rapidly. The rapid increase was attributed to a decrease in emittance below a sample temperature of 200 K.

Preliminary radiative property data were obtained for a Z-93 white coating and a 3M Black Velvet paint. In addition the cyclic technique was used to determine the specific heat of the Z-93 coating.

Lewis Research Center,
National Aeronautics and Space Administration,
Cleveland, Ohio, November 17, 1969,
124-09.

APPENDIX

SYMBOLS

A	amplitude of temperature perturbation during cyclic period, K
A_s	sample area, cm^2
C	constant of integration
c_p	specific heat, J/(g)(K)
I(t)	time varying radiant intensity, $J/(cm^2)(sec)$
I_o	mean radiant intensity, $J/(cm^2)(sec)$
i	amplitude of intensity perturbation, $J/(cm^2)(sec)$
i_m	intensity amplitude at mean temperature during cyclic equilibrium, $J/(cm^2)(sec)$
j	intensity perturbation factor, i/I_o
K	heat-exchange temperature coefficient, J/(sec)(K)
k	extinction coefficient
n	refractive index
q	all heat-exchange terms other than those specified by remaining terms in eq. (1), J/sec
T	test sample temperature, K
$\dot{T}$	time rate of temperature change, K/sec
T_m	mean cyclic temperature of sample, K
t	time, sec
w	test sample weight, g
α	solar absorptance
$\delta( )$	uncertainty interval
ϵ	total hemispherical emittance of sample
ϵ_n	total normal emittance
θ'	time constant of material, sec
λ	wavelength
σ	Stefan-Boltzmann constant, $J/(cm^2)(sec)(K^4)$
σ_e	electrical conductivity, $(ohm\text{-}cm)^{-1}$
φ	phase angle between sample temperature and cyclic incident radiation, rad
ω	cyclic frequency, rad/sec or revolutions per hour (rph)

Subscripts:

b	back surface
c	coating
f	front surface
m	mean temperature
s	standard
1	substrate 1
2	substrate 2

REFERENCES

1. Nelson, K. E.; and Bevans, J. T.: Errors of the Calorimetric Method of Total Emittance Measurements. Measurement of Thermal Radiation Properties of Solids. NASA SP-31, 1963, pp. 55-65.

2. Finkel, Mitchell W.: Portable Reflectometer. Paper 69-599, AIAA, June 1969.

3. Jack, John R.: Technique for Measuring Absorptance and Emittance by Using Cyclic Incident Radiation. AIAA J., vol. 5, no. 9, Sept. 1967, pp. 1603-1606.

4. Spisz, Ernie W.; and Jack, John R.: Experimental Measurements of Thermal Radiation Properties by Cyclic Incident Radiation. NASA TM X-1618, 1968.

5. Jack, John R.; and Spisz, Ernie W.: Thermal Radiative and Electrical Properties of a Cadmium Sulfide Solar Cell at Low Solar Intensities and Temperatures. NASA TN D-4818, 1968.

6. Jack, John R.; and Spisz, Ernie W.: Radiation Properties of a CdS Solar Cell and Various Metals at Space Conditions. Proceedings of the 3rd Space Simulation Conference. Inst. Environmental Sciences, 1968, pp. 99-104.

7. Jack, John R.; and Spisz, Ernie W.: Solar Absorptance and Hemispherical Emittance of Various Metals at Space Conditions. Paper 69-60, AIAA, Jan. 1969.

8. Spisz, Ernie W.; Weigand, Albert J.; Bowman, Robert L.; and Jack, John R.: Solar Absorptances and Spectral Reflectances of 12 Metals for Temperatures Ranging from 300 to 500 K. NASA TN D-5353, 1969.

9. Kline, S. J.; and McClintock, F. A.: Describing Uncertainties in Single-Sample Experiments. Mech. Eng., vol. 75, no. 1, Jan. 1953, pp. 3-8.

10. Gray, Dwight E., ed.: American Institute of Physics Handbook. Second ed., McGraw-Hill Book Co., Inc., 1963.

11. Touloukian, Y. S., ed.: Thermophysical Properties of High Temperature Solid Materials. Vol. 1. Macmillan Co., 1967.

12. Makarounis, O.: Heat Capacity by the Radiant Energy Absorption Technique. Progress in Astronautics and Aeronautics. Vol. 20. G. B. Heller, ed., Academic Press, 1967, pp. 203-218.

13. Heidt, Lawrence J.; and Bosley, David E.: An Evaluation of Two Simple Methods for Calibrating Wavelength and Absorbtance Scales of Modern Spectrophotometers. J. Opt. Soc. Am., vol. 43, no. 9, Sept. 1953, pp. 760-766.

14. Spisz, Ernie W.; and Jack, John R.: Spectral and Operational Characteristics of a High-Intensity Carbon Arc Solar Simulator. NASA TM X-1825, 1969.

15. Anon.: Solar Electromagnetic Radiation. NASA SP-8005, 1965.

16. Terman, Frederick E.; and Pettit, Joseph M.: Electronic Measurements. Second ed., McGraw-Hill Book Co., Inc., 1952.

17. Dunkle, R. V.: Emissivity and Inter-Reflection Relationships for Infinite Parallel Specular Surfaces. Symposium on Thermal Radiation of Solids. NASA SP-55, 1965, pp. 39-44.

18. Siegel, Robert; and Howell, John R.: The Blackbody Electromagnetic Theory, and Material Properties. Vol. 1 of Thermal Radiation Heat Transfer. NASA SP-164, 1968.

19. Domoto, G. A.; Boehm, R. F.; and Tien, C. L.: Predictions of the Total Emissivity of Metals at Cryogenic Temperatures. Rep. TS-68-5, Univ. of California (NASA CR-73264), July 1968.

20. Lyman, Taylor, ed.: Properties and Selection of Metals. Vol. 1 of Metals Handbook. Eighth ed., American Soc. Metals, 1961.

21. Dingle, R. B.: The Anomalous Skin Effect and the Reflectivity of Metals. II. Comparison Between Theoretical and Experimental Optical Properties. Physica, vol. 19, 1953, pp. 348-364.

22. Liebert, Curt H.; and Hibbard, Robert R.: Theoretical Temperatures of Thin-Film Solar Cells in Earth Orbit. NASA TN D-4331, 1968.

NASA-Langley, 1970 —— 33 E-5356

"The aeronautical and space activities of the United States shall be conducted so as to contribute . . . to the expansion of human knowledge of phenomena in the atmosphere and space. The Administration shall provide for the widest practicable and appropriate dissemination of information concerning its activities and the results thereof."

—NATIONAL AERONAUTICS AND SPACE ACT OF 1958

NASA SCIENTIFIC AND TECHNICAL PUBLICATIONS

TECHNICAL REPORTS: Scientific and technical information considered important, complete, and a lasting contribution to existing knowledge.

TECHNICAL NOTES: Information less broad in scope but nevertheless of importance as a contribution to existing knowledge.

TECHNICAL MEMORANDUMS: Information receiving limited distribution because of preliminary data, security classification, or other reasons.

CONTRACTOR REPORTS: Scientific and technical information generated under a NASA contract or grant and considered an important contribution to existing knowledge.

TECHNICAL TRANSLATIONS: Information published in a foreign language considered to merit NASA distribution in English.

SPECIAL PUBLICATIONS: Information derived from or of value to NASA activities. Publications include conference proceedings, monographs, data compilations, handbooks, sourcebooks, and special bibliographies.

TECHNOLOGY UTILIZATION PUBLICATIONS: Information on technology used by NASA that may be of particular interest in commercial and other non-aerospace applications. Publications include Tech Briefs, Technology Utilization Reports and Notes, and Technology Surveys.

Details on the availability of these publications may be obtained from:

SCIENTIFIC AND TECHNICAL INFORMATION DIVISION

NATIONAL AERONAUTICS AND SPACE ADMINISTRATION

Washington, D.C. 20546